LDPC-Coded Modulations: Performance Bounds and a Novel Design Criterion

Michele Franceschini, Gianluigi Ferrari and Riccardo Raheli
Dipartimento di Ingegneria dell'Informazione
University of Parma, Parma, I-43100 Italy
E-mail: mfrance@tlc.unipr.it

Abstract

In this paper, we present a novel design criterion for low-density parity-check (LDPC)-coded modulations based on the concatenation of an LDPC code with a coded modulator (CM) tailored for the specific transmission channel. Although we use an analysis based on extrinsic information transfer (EXIT) charts, we focus on the bit error rate (BER) performance as opposed to the convergence threshold. First, we characterize the convergence behavior of the decoding process as a function of the LDPC code degree distributions. Then, the BER performance is accurately estimated by deriving upper and lower bounds as functions of the extrinsic information.

1 Introduction

Low-density parity-check (LDPC) codes [1], [2] are a coding technique which is gaining increasing attention (from an implementation viewpoint) among the scientific community and the industry. In particular, since LDPC codes exhibit near-capacity performance on a variety of memoryless channels, there is high interest in investigating their performance on practical channels [3].

A simple, although powerful, technique for exploiting LDPC codes over generic channels is based on the use of *LDPC-coded modulations*. This approach is based on the concatenation of an LDPC encoder and a coded modulator (CM) suitable for transmission over the considered channel. This is the approach followed in [4], where an LDPC encoder is concatenated with a multiple-input multiple-output channel modulator. At the receiver, a soft-input soft-output (SISO) module [5] designed for the concatenation of CM and channel iteratively exchanges soft reliabilities with a standard LDPC decoder.

In this paper, we provide insights into the decoding convergence of LDPC-coded modulations. We adopt the receiver block decomposition introduced in [4] and characterize the behavior of the extrinsic information transfer (EXIT) curves [6] in the neighborhood of the point $(1,1)$ in the EXIT chart, i.e., the point of successful decoding convergence. We highlight the dependence of the EXIT curves of the decoding blocks on the LDPC code parameters, i.e., the degree distributions [7], devoting particular attention to the final iterations needed for convergence. A novel bound on LDPC code parameters is given as a necessary condition for decoding convergence. This bound is used in order to justify some previously known features of LDPC codes optimized for specific coded-modulations and channels, such as differentially encoded (DE) phase shift keying (PSK) on additive white Gaussian noise (AWGN) channel and inter-symbol interference (ISI) channels [8], [9].

In order to characterize the extrinsic information evolution on the EXIT chart in terms of BER, we introduce a novel and general upper bound for the BER as a function of the extrinsic information. We then propose a code design criterion, based on the BER evolution with the number of decoding iterations, which can be used to actually design some codes.

This paper is structured as follows. In Section 2, EXIT chart-based convergence analysis of LDPC-coded modulations is reviewed. In Section 3, bounds for the BER as a function of the extrinsic information are derived. In Section 4, the decoding convergence of the BER is analyzed as a function of the LDPC code degree distributions. In Section 5, we introduce a novel code design criterion based on the obtained results. Section 6 concludes the paper.

2 EXIT Chart-Based Analysis

In [4], the authors present an iterative receiver for LDPC codes concatenated with a modulator designed to cope with the specific transmission channel. Following the notation in [8], the receiver can be decomposed into two main blocks: (i) block **A**, comprising a SISO module for the modulator and the set of all variable nodes, denoted as variable node detector (VND) and (ii) block **B**, comprising the set of all check nodes, denoted as check node detector (CND).

Since blocks **A** and **B** exchange iteratively vectors of real valued reliabilities associated with the transmitted LDPC codeword and since for each block these vectors can be computed as a function of the observed received signal and the vector coming from the other block, an analysis of the decoding convergence based on EXIT charts can be performed [4], [6]. The analysis based on EXIT chart tracks the evolution of the mutual information (MI) between the codeword bits and their corresponding reliabilities. It is based on the assumption that the MI associated with the output reliability vector of a block is a function only of the MI associated with the input vector (and a function of the channel statistical description

as well). This assumption represents an accurate approximation and bounds have recently been derived on the MI input-output relation, also referred to as *information combining* [10], [11]. Nevertheless, in practical situations the functional relation assumption turns out to be quite accurate in predicting the system performance [6].

3 Upper and Lower Bounds for the BER

Usually, an EXIT chart-based analysis assumes decoding convergence, i.e., sufficiently low BER, when the MI between the vector of reliabilities and the codeword bits has become equal to 1 [6]. This is because a MI equal to 1 implies that the codeword bits can be expressed as a function of the reliabilities with probability one.

Nevertheless, it is usually impossible for the MI to become equal to 1 with a finite number of decoding iterations. On the other hand, if knowledge of the EXIT curves is available, one can compute the evolution of the MI towards 1 as a function of the number of iterations or, given a maximum number of iterations, one can compute the minimum signal-to-noise ratio[1] (SNR) needed in order to attain a given MI (usually close to 1). Therefore, it becomes useful to have upper and lower bounds on the BER as functions of the MI.

3.1 MI-based Lower Bound for the BER

The reliability values for the codeword bits are usually computed by iterative algorithms in two forms: (i) estimates of the probability of each bit to be equal to 1 and (ii) the corresponding log-likelihood ratio [1]. In general, these reliabilities are random variables (RV) drawn according to a given distribution which is a function of several parameters such as, for example, the SNR, the number of iterations, etc. Typically, a reliability value y is used at the end of the iterative processing to make a decision on the corresponding bit x. This has to be done by applying a proper function $f_{\mathrm{d}}(\cdot)$ to the reliability value.

We assume binary equiprobable transmission of information bits equal to 1 or 0. We denote by $I = I(X;Y)$ the MI between X (a generic bit) and Y (its corresponding reliability), at given values of SNR, number of iterations, etc. A lower bound on the BER, generally denoted as P_{e}, is given by the Fano bound [12]. In fact,

$$\begin{aligned} H(X) &= 1 \\ I(X;Y) &= 1 - H(X|Y) \\ H(P_{\mathrm{e}}) &\geq H(X|Y) \qquad (1) \\ P_{\mathrm{e}} &\geq H^{-1}[1 - I(X;Y)] \qquad (2) \end{aligned}$$

where inequality (1) is the Fano bound applied to a binary RV. The entropy $H(p) \triangleq -p\log(p) - (1-p)\log(1-p)$ is invertible if $p \in (0, 1/2]$. The meaning of inequality (2) is that, even choosing the best decision strategy, the BER cannot be lower than $H^{-1}[1 - I]$.

[1]Here, the SNR is defined, in general terms, as a parameter which completely defines the channel and such that the MI between the input and the output of the channel is a monotonic function of it.

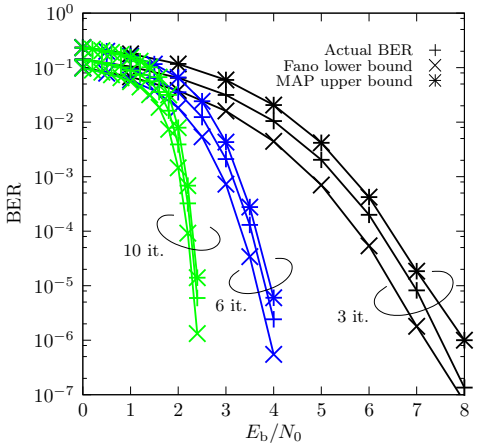

Fig. 1. Actual BER, upper MAP bound and Fano lower bound for a regular (3,6) BPSK modulated LDPC code of codeword length 12000 over an AWGN channel considering 3, 6 and 10 iterations.

3.2 MI-based Upper Bound for the BER

In order to characterize the BER performance, we now derive an upper bound for the BER as a function of the MI. In order to find a useful upper bound for the BER, a decision criterion or, equivalently, a decision function $f_{\mathrm{d}}(\cdot)$ have to be fixed. In many cases of practical interest, the reliability of a bit is represented by the *a posteriori probability* of that bit to be one. Given a set of constraints on the code characteristics, a maximum *a posteriori* (MAP) decision strategy can be implemented straightforwardly simply by deciding for the most probable bit. Thus, we investigate MAP decision of the bit given its reliability. In the general case, this choice requires perfect knowledge of the conditional probability density function (PDF) $f(y|x)$. The following theorem gives an upper bound on the BER, for a given $I(X;Y)$, assuming MAP decision.

Theorem 1: Let X be a binary RV such that $P\{X = 0\} = P\{X = 1\} = 1/2$, Y be a RV and $f(y|x)$ be the conditional PDF of Y given X. Let

$$\hat{x} = \operatorname*{argmax}_x f(y|x).$$

Given the conditional entropy $H(X|Y) = 1 - I(X;Y)$, then

$$P_{\mathrm{e}} = P\{X \neq \hat{x}\} \leq \frac{H(X|Y)}{2}.$$

Proof: See the Appendix. ■

In Fig. 1, the obtained bounds, along with the actual BER performance versus the bit SNR E_{b}/N_0, are shown considering a regular (3,6) LDPC code with codeword length 12000 [1]. The modulation format is binary shift phase keying (BPSK). The considered numbers of iterations are 3, 6 and 10. The bounds clearly describe the behavior of the BER curve. Thus, the convergence of the MI has useful implications on the convergence of the BER. This finding will be exploited in the next sections.

4 Decoding Convergence

In Fig. 2, the decoding trajectory of the MI on a generic EXIT chart is shown, referring to the decoding scheme

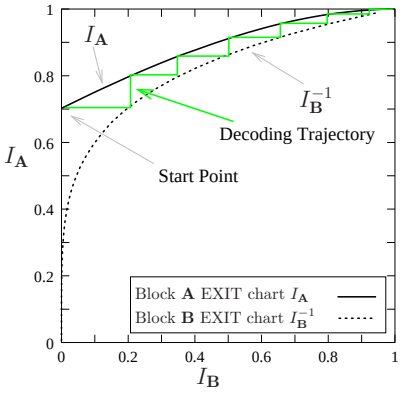

Fig. 2. Decoding trajectory on an EXIT chart-based LDPC-coded modulation decoding analysis.

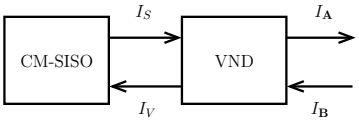

Fig. 3. Representation of block **A**.

in [4]. The upper curve is the EXIT curve of block **A**, which comprises the CM-SISO block and the VND. The lower curve is the inverse of EXIT curve of the block **B**, which comprises the CND. It is easily recognized that in order for the MI to converge to 1, the EXIT curve of block **A**, i.e., $I_{\mathbf{A}}(I)$, and the inverse of the EXIT curve of block **B**, i.e., $I_{\mathbf{B}}^{-1}(I)$, must satisfy the following condition:

$$I_{\mathbf{A}}(I) > I_{\mathbf{B}}^{-1}(I) \qquad 0 < I < 1\,. \tag{3}$$

Moreover, given the behavior of $I_{\mathbf{A}}(I)$ and $I_{\mathbf{B}}^{-1}(I)$ in proximity of the point $(1,1)$, one can completely characterize the convergence of the MI as a function of the number of iterations.

The degree distributions of an LDPC code are defined as a couple of polynomials $\lambda(x) = \sum_i \lambda_i x^{i-1}$ and $\rho(x) = \sum_j \rho_j x^{j-1}$, where the coefficients $\{\lambda_i\}$ and $\{\rho_j\}$ denote the fraction of edges in the LDPC code graph connected to degree-i variable nodes and degree-j check nodes, respectively [7].

In Fig. 3, a representation of block **A** is given and the MI related to the reliability vectors involved in the computation is shown. In particular, the functional relationships of the MI values is as follows: $I_{\mathbf{A}}$ is a function of $I_{\mathbf{B}}$ and $I_{\mathbf{S}}$; $I_{\mathbf{S}}$ is a function of I_V, which is also a function of $I_{\mathbf{B}}$

$$I_{\mathbf{A}} = I_{\mathbf{A}}(I_{\mathbf{B}}, I_S(I_V(I_{\mathbf{B}}))).$$

In order to characterize the decoding convergence, we now compute the first order Taylor series expansion of $I_{\mathbf{A}}$ as a function of $I_{\mathbf{B}}$. The derivative of $I_{\mathbf{A}}$ is as follows

$$\frac{\mathrm{d}I_{\mathbf{A}}}{\mathrm{d}I_{\mathbf{B}}} = \frac{\partial I_{\mathbf{A}}}{\partial I_{\mathbf{B}}} + \frac{\partial I_{\mathbf{A}}}{\partial I_S}\frac{\partial I_S}{\partial I_{\mathbf{B}}}. \tag{4}$$

On the other hand, $I_{\mathbf{A}}$ can be expressed as a linear combination of terms depending on $I_{\mathbf{B}}$ and I_S, weighted by the coefficients $\{\lambda_i\}$ [4], [13]:

$$I_{\mathbf{A}} = \sum_i \lambda_i I_V^{(i)}(I_{\mathbf{B}}, I_S) \tag{5}$$

where $I_V^{(i)}$ is the EXIT function associated with a generic degree-i variable node. In the process of obtaining the reliabilities associated to I_V, at the input of the CM-SISO block, a generic degree-i variable node acts as a degree-$(i+1)$ variable node with no *a priori* information, i.e., with input *a priori* probability equal to $1/2$. This is due to the symmetry of the computation of variable nodes with respect to the messages coming from both the graph and the channel, i.e., the *a priori* probability [1]. As a consequence,

$$I_V = \sum_k \lambda_k I_V^{(k+1)}(I_{\mathbf{B}}, 0)\,. \tag{6}$$

Substituting (5) and (6) into (4), one obtains

$$\frac{\mathrm{d}I_{\mathbf{A}}}{\mathrm{d}I_{\mathbf{B}}} = \sum_i \lambda_i \left[\frac{\partial I_V^{(i)}}{\partial I_{\mathbf{B}}} + \frac{\partial I_V^{(i)}}{\partial I_S}\frac{\partial I_S}{\partial I_V}\sum_k \lambda_k \frac{\partial I_V^{(k+1)}}{\partial I_{\mathbf{B}}}\right] \tag{7}$$

where $\frac{\partial I_S}{\partial I_V}$ denotes the derivative of the CM-SISO EXIT curve with respect to the MI I_V as its *a priori* input.

The block **B** is formed by the CND. As considered for block **A**, the EXIT curve of block **B** can be written as a weighted linear combination of the degree distribution $\{\rho_j\}$ as follows [4], [13]:

$$I_{\mathbf{B}} = \sum_j \rho_j I_C^{(j)}(I_{\mathbf{A}}) \tag{8}$$

where $I_C^{(j)}$ denotes the EXIT function associated with a generic degree-j check node. From (8), one obtains that the derivative of $I_{\mathbf{B}}$, with respect to $I_{\mathbf{A}}$, can be written as

$$\frac{\mathrm{d}I_{\mathbf{B}}}{\mathrm{d}I_{\mathbf{A}}} = \sum_j \rho_j \frac{\mathrm{d}I_C^{(j)}}{\mathrm{d}I_{\mathbf{A}}}(I_{\mathbf{A}}). \tag{9}$$

In [14], it is shown that the reliability distributions in the convergence region, i.e., around the point $(1,1)$ in the EXIT charts, due to a large variance, tend to behave like the distributions found for a binary erasure channel (BEC). In other words, the reliabilities tend to group into high, i.e., corresponding to sure decisions, and low, i.e., erasure-like. This fact suggests that in the convergence region one can approximate the information transfer functions $I_V^{(i)}(\cdot,\cdot)$ and $I_C^{(j)}(\cdot)$ with the BEC information combining functions for a single parity check node and a single variable node [10], [15]:

$$I_V^{(i)}(I_{\mathbf{B}}, I_S) \simeq 1-(1-I_S)(1-I_{\mathbf{B}})^{i-1} \tag{10}$$

$$I_C^{(j)}(I_{\mathbf{A}}) \simeq I_{\mathbf{A}}^{j-1}. \tag{11}$$

The particular cases corresponding to $I_C^{(2)}$, $I_V^{(1)}(I_{\mathbf{B}}, I_S)$, and $I_V^{(2)}(I_{\mathbf{B}}, 0)$ need no approximation, since in these three particular cases the check and variable nodes act as identity blocks:

$$\begin{aligned} I_C^{(2)}(I_{\mathbf{A}}) &= I_{\mathbf{A}} \\ I_V^{(1)}(I_{\mathbf{B}}, I_S) &= I_S \\ I_V^{(2)}(I_{\mathbf{B}}, 0) &= I_{\mathbf{B}}. \end{aligned} \tag{12}$$

We remark that from (5), (8), (11) and (13), one can conclude the following facts:

- $I_{\mathbf{B}}(1) = 1$
- $I_{\mathbf{A}}(1, I_S) = 1 - \lambda_1 + I_S\lambda_1$ which is lower than 1 if $\lambda_1 > 0$ and $I_S < 1$ for $I_{\mathbf{B}} = 1$.

In other words, since $I_{\mathbf{B}}(1) = 1$, it must be either $\lambda_1 = 0$ or $I_S = 1$ for $I_{\mathbf{B}} = 1$, for the decoding process to converge.

We now substitute the previously given approximations (10) and (11) into (7) and (9) in order to find the first order Taylor series approximation of the EXIT curves of blocks **A** and **B** at the point $(1, 1)$:

$$\frac{\partial I_V^{(i)}}{\partial I_{\mathbf{B}}}(1, I_S) = \begin{cases} 0 & i = 1 \\ 1 - I_S & i = 2 \\ 0 & \text{otherwise} \end{cases}$$

$$\frac{\partial I_V^{(i)}}{\partial I_S}(1, I_S) = \begin{cases} 1 & i = 1 \\ 0 & \text{otherwise.} \end{cases}$$

Substituting these relations into (7), one obtains

$$\frac{\mathrm{d}I_{\mathbf{A}}}{\mathrm{d}I_{\mathbf{B}}}(1) = \lambda_1^2 \frac{\partial I_S}{\partial I_V} + \lambda_2(1 - I_S)\,. \qquad (13)$$

Moreover, from (9) and (11) it follows that

$$\frac{\partial I_{\mathbf{B}}}{\partial I_{\mathbf{A}}}(1) \simeq \sum_j (j-1)\rho_j\,.$$

The derivative of the inverse of the EXIT curve of block **B** is therefore given by

$$\frac{\partial I_{\mathbf{B}}^{-1}}{\partial I_{\mathbf{A}}}(1) = \frac{1}{\sum_j (j-1)\rho_j}\,.$$

In order for the decoding process to converge, (3) must hold and the derivative of the two functions must satisfy the following inequality:

$$\lambda_1^2 \frac{\partial I_S}{\partial I_V} + \lambda_2(1 - I_S) < \frac{1}{\sum_j (j-1)\rho_j}\,. \qquad (14)$$

This bound gives a relation between λ_1, λ_2, $I_S(I_V)$ and $\{\rho_j\}$, which represents a necessary condition that an LDPC-coded modulation system must satisfy in order to reach decoding convergence.

In the following, some examples of application of the obtained results are given.

Example 1 Consider a single LDPC-coded communication system with BPSK transmission over an AWGN channel. In this case, the CM block is simply the BPSK modulator and the CM-SISO block could consist of a block performing a symbol-by-symbol conversion from the received sample domain to the log-likelihood *a priori* probability domain. Since no side information is needed by the CM-SISO block to perform this task, the associated EXIT curve I_S is a constant function of the MI I_V of the reliabilities passed by the VND to the CM-SISO block. This is shown explicitly in Fig. 4, obtained through computer simulations. Since $I_S(1) < 1$, it must hold that $\lambda_1 = 0$. Moreover, the bound (14) becomes

$$\lambda_2 < \frac{1}{(1 - I_S)\sum_j (j-1)\rho_j}\,.$$

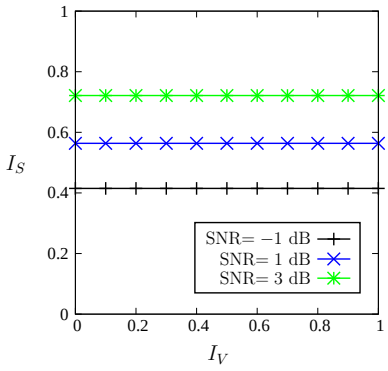

Fig. 4. EXIT curve I_S, as a function of I_V, of the CM-SISO block for BPSK and AWGN channel.

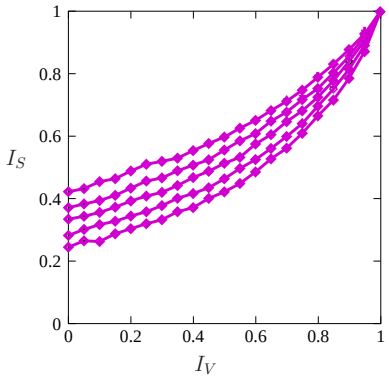

Fig. 5. EXIT curves I_S, as a function of I_V, of the CM-SISO block for DE-QPSK and AWGN channel. The various curves correspond to different values (equally spaced by 0.5 dB) of SNR, from 0 dB (bottom curve) to 2 dB (top curve).

This condition can be directly related to the following stability condition given in [7]:

$$\lambda_2 \sum_j (j-1)\rho_j < e^{\frac{1}{2\sigma^2}}$$

where σ^2 is variance of the additive noise sample and $1/\sigma^2$ is the SNR.

Example 2 In [8], code optimization for DE M-ary PSK (MPSK) LDPC-coded modulations is considered. The optimized LDPC codes show a structure very different from that of standard LDPC codes for the AWGN channel. In particular, the fraction of degree-2 variable node λ_2 is significantly increased. In Fig. 5, EXIT curves for a DE-QPSK CM-SISO block are shown, for various values of the SNR. One can notice that $I_S(1) = 1$. Therefore, given that in the optimized codes $\lambda_1 = 0$, the bound (14) becomes

$$\lambda_2 < \frac{1}{(1 - I_S)\sum_j (j-1)\rho_j}$$

where the presence of the term $(1 - I_S) \simeq 0$ at the denominator implies that the bound on λ_2 is relaxed, thus allowing a larger optimized value for this coefficient. The significant difference between the obtained optimized degree distributions and the degree distributions of an LDPC code for the AWGN channel suggests that the

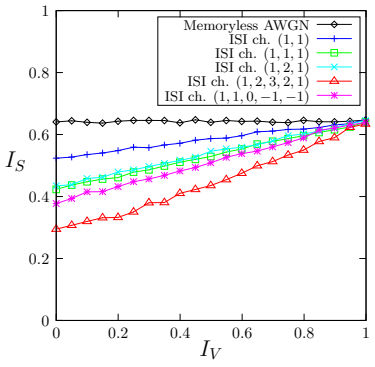

Fig. 6. EXIT chart I_S of the CM-SISO block for 4PSK and several ISI channels.

extended λ_2 range has been exploited. Since the optimization algorithm in [8] optimizes the global convergence threshold, it is very likely that the increased range for λ_2 allows to achieve a better decoding threshold at the expense of decoding convergence speed.

Example 3 In [9], [16], examples of optimized LDPC codes are given both for an AWGN channel affected by inter-symbol interference (ISI) and for a partial response (PR) channel. In [9], it is shown how optimized codes may differ from AWGN LDPC codes if the channel response is long enough. In Fig. 6, several EXIT curves of CM-SISO blocks for several ISI channels are shown. In particular, the SNR is fixed and ISI channels with impulse response coefficients (the impulse energy normalization factor is not shown) $(1,1)$, $(1,1,1)$, $(1,2,1)$, $(1,2,3,2,1)$ and $(1,1,0,-1,-1)$ are considered. As noted in [9], a linear behavior of the EXIT curves is easily recognized, as well as the increase of the slope of the EXIT curves for longer channel impulse response length. Since $I_S(1) < 1$, degree-1 variable nodes are not allowed. The bound on λ_2 is equal to that for BPSK transmission over the AWGN channel. Nevertheless, due to the reduced 4PSK input channel capacity of the ISI channels, the SNR needed to achieve convergence at a given code rate is higher that that needed for the AWGN channel. This leads to a larger $I_S(1)$ value and, therefore, to a larger allowed λ_2 value, according to

$$\lambda_2 < \frac{1}{(1-I_S)\sum_j (j-1)\rho_j} .$$

This result can be verified by optimizing LDPC codes for ISI or PR channels. The resulting codes exhibit high values for λ_2 in the case of channels with long impulse response [9].

5 A Novel Design Criterion

The results obtained in Section 3 and Section 4 suggest that knowledge of EXIT functions in the proximity of the point $(1,1)$ of the EXIT charts can be exploited to design LDPC codes for LDPC-coded modulations. In particular, since EXIT charts enable analysis and design of convergence of MI and since there are bounds which "link" the MI to the BER, it is possible to design LDPC codes for a given asymptotic BER convergence as a function of the number of iterations.

The considered analysis does not take into account *cycles* in the code graph [1], [2]. Cycles have a major impact on three important LDPC codes parameters: (i) the codeword length, (ii) the maximum number of iterations and (iii) the maximum allowed node degree. In general, decoding tends to be close to optimal if (i) the codeword length is large, (ii) the number of iterations needed for convergence is kept low, and (iii) the maximum nodes degree is low.

Given these considerations, a new LDPC design criterion can be based on the convergence of the MI at a given value in a given number of iterations. If the number of iterations is low, convergence is likely to be guaranteed also for short codeword lengths. We now provide the reader with an example of application of the proposed criterion.

Example 4 Given a system such that both the derivatives, evaluated in 1, of the EXIT functions of blocks **A** and **B** are known and non-zero, the convergence law of the decoding process can be derived as follows.

In the neighborhood of 1 the EXIT curves $I_{\mathbf{A}}$ and $I_{\mathbf{B}}$ can be approximated by their first-order Taylor series expansions:

$$\begin{aligned} I_{\mathbf{A}}(I) &\simeq 1 - a(1-I) \\ I_{\mathbf{B}}(I) &\simeq 1 - b(1-I) \end{aligned}$$

where

$$\begin{aligned} a &\triangleq \lambda_1^2 \frac{\partial I_S}{\partial I_V} + \lambda_2 (1 - I_S(1)) \\ b &\triangleq \sum_j (j-1)\rho_j . \end{aligned}$$

The recursion characterizing the decoding behavior is

$$\begin{aligned} I_{2n+1} &= 1 - a(1 - I_{2n}) \\ I_{2n+2} &= 1 - b(1 - I_{2n+1}) . \end{aligned} \tag{15}$$

Substituting the variable $H_n = 1 - I_n$ in the recursion (15), one obtains

$$\begin{aligned} H_{2n+1} &= aH_{2n} \\ H_{2n+2} &= bH_{2n+1} . \end{aligned} \tag{16}$$

The start point of the recursion (15) is I_{2n_0} (or H_{2n_0} for recursion (16)) where n_0 is the number of iterations needed to reach the convergence region, i.e., the region in which the first order Taylor series approximation for $I_{\mathbf{A}}$ and $I_{\mathbf{B}}$ holds. By solving (16), one gets

$$H_{2(n+n_0)} = (ab)^n H_{2n_0}$$

and

$$I_{2(n+n_0)} = 1 - (ab)^n (1 - I_{2n_0})$$

which is the MI at the (n_0+n)-th iteration. Applying the bound (1) one obtains

$$\mathrm{BER}_{n+n_0} \leq (ab)^n \frac{H_{n_0}}{2} \tag{17}$$

where BER_n denotes the BER after n iterations. Inequality (17) allows the computation of the minimum number of additional iterations to perform, starting from n_0, in order to obtain the desired BER, denoted as $\mathrm{BER}^{\mathrm{target}}$:

$$n_{\min} = \frac{\log(2\mathrm{BER}^{\mathrm{target}}/H_{n_0})}{\log(ab)}.$$

An alternative, more useful, viewpoint could be the design of the degree distributions. Towards this end, by simple manipulation of (17) one obtains

$$ab \leq \left(\frac{2\mathrm{BER}^{\mathrm{target}}}{H_{n_0}}\right)^{1/n}$$

and, therefore,

$$\left[\lambda_1^2 \frac{\partial I_S}{\partial I_V} + \lambda_2(1-I_S(1))\right] \sum_j (j-1)\rho_j \leq \left(\frac{2\mathrm{BER}^{\mathrm{target}}}{H_{n_0}}\right)^{1/n}$$

which represents a design constraint guaranteeing convergence to the desired $\mathrm{BER}^{\mathrm{target}}$ in $n+n_0$ iterations.

6 Concluding Remarks

In this paper, we have presented a novel bound for the BER performance of LDPC-coded modulations based on MI. This bound can be used to "link" an EXIT chart-based analysis with the BER performance. The EXIT chart-based analysis of LDPC-coded modulations has been carried out focusing on the convergence region, i.e., the point $(1,1)$ of the EXIT chart. The decoding convergence behavior has been characterized as a function of the LDPC code degree distributions. This analysis has led to a new bound for the degree distributions which can be interpreted as a practical generalization of the bound given in [7] for LDPC codes transmitted over memoryless channels.

Based on the above considerations and results, a novel LDPC code design criterion has been proposed. This criterion gives a new bound for the coefficients of the LDPC code degree distributions in order to obtain convergence within a specified number of iterations. This may have important implications in the design of LDPC codes with short codeword length.

Appendix

The MAP strategy entails a decision for $\hat{x}$, as a function of y, according to

$$\hat{x} = \underset{x}{\mathrm{argmax}}\, P\{X=x|Y=y\}.$$

This implies the following relation for the probability of occurrence of the error event $E=\{X\neq\hat{x}\}$:

$$\begin{aligned} P\{E|Y=y\} &= 1-\max_x P\{X=x|Y=y\} \\ &= \min_x P\{X=x|Y=y\} \end{aligned} \tag{18}$$

which is, obviously, a number lower than or equal to $1/2$. Considering (18), one can conclude that

$$H(X|Y=y) = H(P\{X=x|Y=y\}) = H(P\{E|Y=y\})$$

Therefore, given $H(X|Y=y)$, assuming that the MAP strategy is used, $P\{E|Y=y\}$ can be written as

$$P\{E|Y=y\} = H^{-1}[H(X|Y=y)] \tag{19}$$

where $H^{-1}(\cdot)$ is the inverse of the function $H(p)$ for $p\in(0,\frac{1}{2}]$. The following derivation, which proves the theorem, holds:

$$\begin{aligned} P_{\mathrm{e}} &= E_y\{P\{E|Y=y\}\} \\ &= E\{H^{-1}[H(X|Y=y)]\} &(20)\\ &\leq \frac{H(X|Y)}{2} &(21) \end{aligned}$$

where (20) follows from (19) and (21) follows from the fact that $H^{-1}(x) < x/2$, $\forall x: 0\leq x<1$.

References

[1] R. G. Gallager, *Low-Density Parity-Check Codes*. Cambridge, MA: MIT Press, 1963.

[2] T. Richardson and R. Urbanke, "The capacity of low density parity check codes under message passing decoding," *IEEE Trans. Inform. Theory*, vol. 47, pp. 599–618, February 2001.

[3] M. Franceschini, G. Ferrari, and R. Raheli, "Does the performance of LDPC codes depend on the channel?" in *Proc. IEEE Symposium on Information Theory and Applications* (ISITA), Parma, Italy, October 2004, pp. 55–59.

[4] S. ten Brink, G. Kramer, and A. Ashikhmin, "Design of low-density parity-check codes for modulation and detection," *IEEE Trans. Commun.*, vol. 52, no. 4, pp. 670–678, April 2004.

[5] S. Benedetto, D. Divsalar, G. Montorsi, and F. Pollara, "Soft-Input Soft-Output modules for the construction and distributed iterative decoding of code networks," *European Trans. Telecommun.*, vol. 9, no. 2, pp. 155–172, March/April 1998.

[6] S. ten Brink, "Convergence of iterative decoding," *IEE Electronics Letters*, vol. 35, pp. 1117–1119, 24th June 1999.

[7] T. Richardson, A. Shokrollahi, and R. Urbanke, "Design of capacity-approaching irregular low-density parity check codes," *IEEE Trans. Inform. Theory*, vol. 47, pp. 619–637, February 2001.

[8] M. Franceschini, G. Ferrari, R. Raheli, and A. Curtoni, "Serial concatenation of ldpc codes and differential modulations," *IEEE J. Select. Areas Commun.*, vol. 23, no. 9, pp. 1758–1768, September 2005.

[9] M. Franceschini, G. Ferrari, and R. Raheli, "EXIT chart-based design of LDPC codes for inter-symbol interference channels," in *Proc. IST Mobile Summit*, Dresden, Germany, June 2005.

[10] I. Land, S. Huettinger, P. A. Hoeher, and J. H. Huber, "Bounds on information combining," *IEEE Trans. Inform. Theory*, vol. 51, no. 2, pp. 612–619, February 2005.

[11] I. Sutskover, S. Shamai, and J. Ziv, "Extremes of information combining," *IEEE Trans. Inform. Theory*, vol. 51, no. 4, pp. 1313–1325, April 2005.

[12] T. M. Cover and J. A. Thomas, *Elements of Information Theory*. New York: John Wiley & Sons, Inc., 1991.

[13] M. Ardakani and F. R. Kschischang, "A more accurate one-dimensional analysis and design of irregular LDPC codes," *IEEE Trans. Commun.*, vol. 52, no. 12, pp. 2106–2114, December 2004.

[14] J. Huber, I. Land, and P. A. Hoeher, "Information combining: Models, bounds, and applications," in *Proc. Int. Symp. Inform. Theory and Applic.* (ISITA'04), Parma, Italy, October 2004.

[15] A. Ashikhmin, G. Kramer, and S. ten Brink, "Extrinsic information transfer functions: model and erasure channel properties," *IEEE Trans. Inform. Theory*, vol. 50, no. 11, pp. 2657–2673, November 2004.

[16] A. Kavčić, X. Ma, and M. Mitzenmacher, "Binary intersymbol interference channels: Gallager codes, density evolution, and code performance bounds," *IEEE Trans. Inform. Theory*, vol. 49, no. 7, pp. 1636–1652, July 2003.